ENCAPSULATION OF Fe_2O_3 NANOPARTICLES IN PERIODIC MESOPOROUS MATERIALS

S.E. Dapurkar and P. Selvam

Department of Chemistry, Indian Institute of Technology-Bombay, Powai, Mumbai 400 076, India

Abstract. The preparation of iron oxide nanoparticles in the mesopore of silicate MCM-41 and MCM-48 materials is demonstrated. The encapsulation of iron oxy-hydroxides was carried out at room temperature by incipient wetness method and the corresponding oxides were obtained by calcination. This process not only resulted in entrapment of iron oxy-hydroxides / oxides in the mesopores but also led to isomorphous substitution of trivalent iron in the silicate framework. The encapsulated nanoparticles exhibit superparamagnetism while the substituted iron shows paramagnetic behavior. The above is ascertained by using various techniques viz., X-ray diffraction (XRD), diffuse reflectance ultraviolet-visible (DRUV-VIS), electron paramagnetic resonance (EPR), Mössbauer, and magnetic susceptibility measurements.

1. INTRODUCTION

Microporous materials can exclusively be used for a variety of applications such as sorbents, ion-exchangers, shape selective catalysts and molecular hosts [1,2]. The well-defined and uniform pore systems act as a suitable reaction chamber for controlled assembling of nanosized metal/metal oxides [1,2]. In recent years, there is a considerable interest in the study of metal/metal oxides nanoparticles/ nanoclusters formed in microporous materials as they can potentially be used in optics, electronics, sensors and photocatalysis [3,4]. However, the restricted pore size (< 2 nm) limits their applicability for such purposes. On the other hand, the discovery [5] of the periodic mesoporous materials (e.g., MCM-41 and MCM-48) has opened new opportunities in the development of nanomaterials [6]. The unique flexibility in terms of synthesis conditions, pore size tunning (2-20 nm), high internal surface area (700-1400 $m^2 \cdot g^{-1}$), framework substitution, etc. has created new avenues not only as host materials but also in the area of catalysis, advanced materials, environmental pollution control strategies, separation process, etc. [7].

Recently, Iwamoto et al. [8] and Fröba et al. [9] have reported the encapsulation of Fe_2O_3 nanoparticles in MCM-41 and MCM-48 silicates, respectively. However, the interpretation of experimental data requires careful analysis owing to the complicated nature of the host materials having various possible sites (e.g., non-framework, extra-framework and framework) of accommodating the guest materials even at ambient condition. In view of the fact that the possibility of isomorphous substitution of heterometal ions in the mesoporous silicate materials, viz., AlMCM-41 [10], AlMCM-48 [11], FeMCM-41 [12] and FeHMS [13], under such conditions warrants the interpretation of nanoparticles in the mesopores. Furthermore, FeMCM-41 prepared under hydrothermal conditions showed evidence for the encapsulation as well as isomorphous substitution of trivalent iron in the MCM-41 [14]. In view of the above, in the present study, we have undertaken a systematic investigation of encapsulation of iron oxides nanoparticles and their influence in the framework substitution in MCM-41 and MCM-48 structure. For a comparison, we have also synthesized and characterized the ferrisilicate analogous of MCM-41 (FeMCM-41) and MCM-48 (FeMCM-48).

Corresponding author: P.Selvam, e-mail: selvam@iitb.ac.in

2. EXPERIMENTAL

The following chemicals were used for the preparation of various mesoporous MCM-41 and MCM-48 silicates and their corresponding ferrisilicates, *viz.*, FeMCM-41 and FeMCM-48, as well as for the loading experiments: Fumed silica (SiO_2), tetraethyl orthosilicate (TEOS), tetramethylammonium hydroxide (TMAOH), cetytrimethylammonium bromide (CTAB), sodium hydroxide (NaOH), iron nitrate nonahydrate ($Fe(NO_3)_3 \cdot 9H_2O$), sulfuric acid (H_2SO_4), bulk iron oxide (Fe_2O_3) and distilled water. All the mesoporous materials were synthesized hydrothermally according to a similar procedure described elsewhere [15-17]. Incipient wetness method was adopted for the loading experiments with 0.008 - 0.1 *M* aqueous iron nitrate at pH < 2 and room temperature, as per the procedure outlined earlier [16, 17]. The resulted loaded samples are designated as FeO(OH)/MCM-41 and FeO(OH)/MCM-48. Unless it is stated, the samples studied in this work were prepared with 0.008 *M* loading of iron nitrate solution. In order to ensure the formation of the iron oxide particles, the loaded samples were calcined at 773K in air for 8 h. They are represented as Fe_2O_3 /MCM-41 and Fe_2O_3 /MCM-48, respectively.

Powder X-ray diffraction (XRD) was recorded in the region (1.5-80°) on Siemens diffactometer using a Ni filitered Cu K_α radiation. Diffuse reflectance ultraviolet-visible (DRUV-VIS) spectra were recorded (200–700 nm) on UV-260 Shimadzu spectrometer. Electron paramagnetic resonance (EPR) spectra were recorded on a Varian (E-line Century series E-112) spectrophotometer. The iron content of the samples was determined (0.7-2.5 wt. %) by inductively coupled plasma-atmoic emission spectroscopy (ICP-AES) on a Labtam plasma lab 8440 equipment.

3. RESULTS AND DISCUSSION

Fig. 1 shows the XRD patterns of encapsulated Fe_2O_3 in MCM-41 and MCM-48, typical of mesoporous (hexagonal) MCM-41and (cubic) MCM-48 structures [5,7], which indicate the intactness of structures even after loading. It is, however, interesting to note that the d_{hkl} values for the loaded samples were shifted to higher *d*-values or lower 2θ values (d_{211} = 37.80 Å for FeO(OH)/MCM-48; d_{211} = 37.61 Å for Fe_2O_3/ MCM-48) as compared to the siliceous analogue (d_{211} = 36.40 Å for MCM-48). A similar observation was also made eariler for FeO(OH)/MCM-41 and Fe_2O_3/MCM-41 [17]. The increase in the *d*-values of the loaded samples could
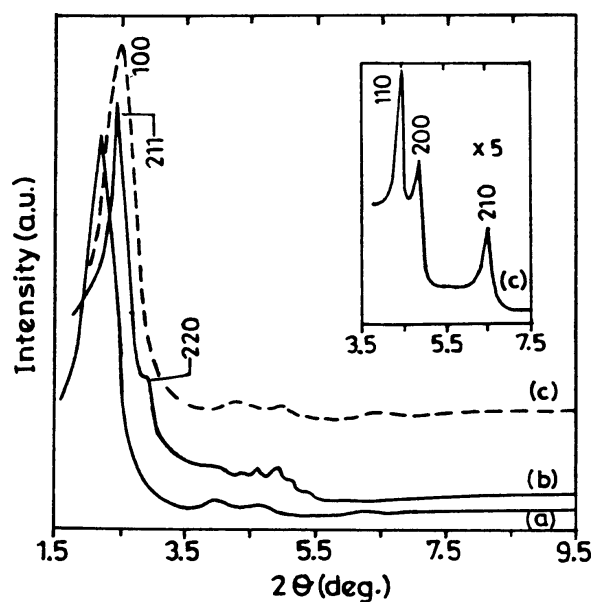

Fig. 1. XRD patterns of: (a) Fe_2O_3/MCM-41; (b) Fe_2O_3/MCM-48; (c) Fe_2O_3/MCM-41 (0.01 M).

be attributed to the possible (isomorphous) substitution of trivalent iron for tetravalent silicon [15,16,20] as the crystal radii of these ions in tetrahedral coordination (r_{Si}^{4+} = 0.40 Å and r_{Fe}^{3+} = 0.63 Å) [18] favor such an observation. The high angle diffraction patterns of unloaded and iron loaded samples (at < 0.01 *M*) in the range 10-80° (not shown here), shows only diffuse peaks of noncrystalline silica framework. However, at higher iron concentration weak reflections corresponding to iron oxides were observed, suggesting that beyond certain concentration the iron oxyhydroxides / oxides particles agglomerated on the external surface.
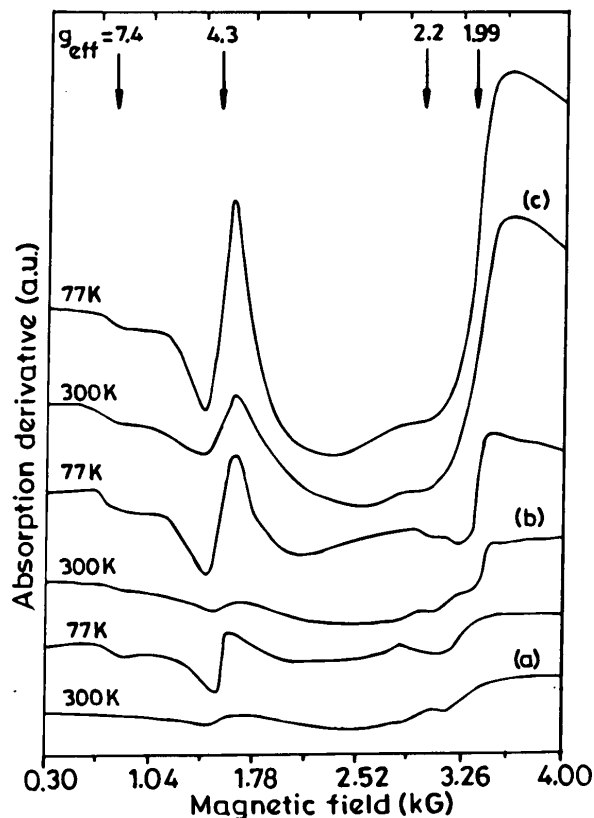
Fig. 2 depicts the DRUV-VIS spectra of various iron-containing samples. The bulk Fe_2O_3 shows a broad band in the range 320-700 nm, having strong maxima at 560 nm (Fig. 2f). On the hand, the loaded Fe_2O_3/MCM-41 and Fe_2O_3/MCM-48 show absorption bands at ~ 250 nm (Fig. 2a and 2b), which could be assigned to Fe_2O_3 nanoparticles inside the mesopores, owing to the quantum size effect. However, due care must be taken in interpreting such bands as these bands can also be assigned to tetrahedral Fe^{3+} in FeMCM-41, FeMCM-48 and FeHMS [14,16,19,20], see also Fig. 2e. The occurrence of these absorption maxima can thus be assigned to both entrapped iron oxide nanoparticles and framework iron [17]. However, upon increase in loading (= 0.01 *M*) a strong absorption in the range of 320-550 nm was observed in addition to 250 nm band, attributed to the agglomerated Fe_2O_3 on the surface [8,16], see Fig. 2c and 2d.
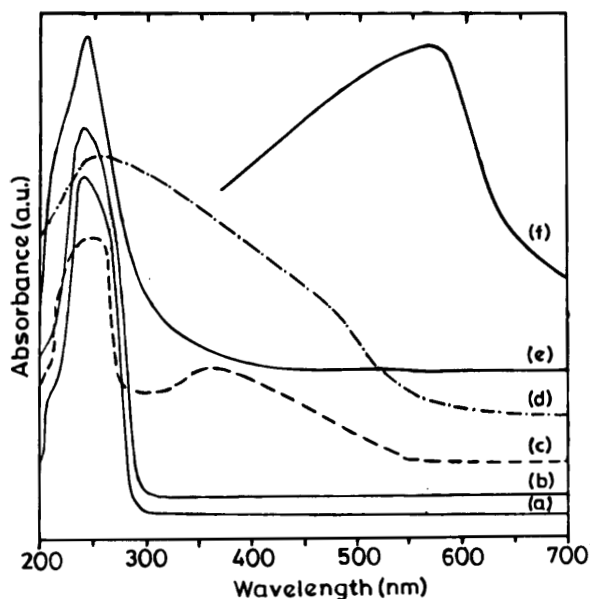
Fig. 2. DRUV-VIS spectra of: (a) Fe_2O_3/MCM-41; (b) Fe_2O_3/MCM-48; (c) Fe_2O_3/MCM-41 (0.01 M); (d) Fe_2O_3/MCM-41 (0.1 M); (e) FeMCM-48; (f) bulk Fe_2O_3.

Fig. 3. EPR spectra (300 and 77K) of: (a) Fe_2O_3/ MCM-41; (b) Fe_2O_3/MCM-48; (c) FeMCM-48.

Fig. 3 presents the EPR spectra of various samples. It can be seen from the figure that three different signals appears at various g_{eff} values (4.20, 2.23 and 1.99) corresponding to the presence of three distinct environments around the trivalent iron. On the basis of earlier assignments [16,17,19,21,22], the signal at 4.20 is ascribed to Fe^{3+} in distorted tetrahedral framework sites, and the signal at 1.99 is attributed to trivalent iron in both framework and extra-framework sites. The weak signal centered at 2.1-2.3 is also prominent at 77K and is attributed to non-framework (superparamagnetic) iron oxy-hydroxides/oxide nanoparticles located in the pores [17,21-24]. Although, the room temperature spectra of the loaded samples (Fig. 3a-3b) show weak and broad signals, the corresponding spectra at 77K show sharp and intense signals at 4.20 and 1.99. The intensity ratio ($I_{4.3}/I_{1.99}$) for Fe_2O_3/MCM-41 (1.17) and for Fe_2O_3/ MCM-48 (1.15) at 77K, where as for FeMCM-41 (0.62) and FeMCM-48 (0.63), indicating the partial substitution of trivalent iron in the further cases. Thus, the loading of trivalent iron in mesoporous matrix results not only as nanoparticles but also present in the framework sites of MCM-41 and MCM-48 structures.

Preliminary, Mössbauer studies on loaded (Fe_2O_3/MCM-41) at room temperature shows a singlet, which is assigned to high spin (paramagnetic)

Fe^{3+} in tetrahedral framework sites as well as iron oxy-hydroxides/oxides (superparamagnetic) particles in the mesopore. However, upon lowering the temperature (15K), a sextet pattern, in addition to the paramagnetic contribution, characteristic of superparamagnetic iron oxides nanoparticles appears [14,17]. This observation is well supported by the temperature dependence of the susceptibility measurements [14]. Further, work is in progress in order to understand the exact nature of the nanoparticles.

4. CONCLUSION

From above study, it can be deduced that the observed blue shift in the absorption edge of the loaded FeO(OH)/Fe_2O_3 in MCM-41 and MCM-48 samples alone cannot be taken as a finger print for the quantum size effect as the isomorphously substituted trivalent iron in the mesoporous matrix can also absorb in the same region. EPR, Mössbauer and magnetic susceptibility measurements give evidence for the existence of trivalent iron in the framework sites as well as in the mesopores of MCM-41 and MCM-48.

ACKNOWLEDGEMENT

REFERENCES

[1] G.D. Stucky and J.E.M. Dougall // *Science* **247** (1990) 669.

[2] N. Herron, Y. Wang, M.M. Eddy, G.D. Stucky, D.E. Cox, K. Moller and T. J. Bein // *J. Am. Chem. Soc.* **111** (1989) 530.

[3] X. Zhang, S.A. Janekhe and J. Perlstein // *Chem. Mater.* **8** (1996) 1571.

[4] J.H. Fendler // *Chem. Mater.* **8** (1996) 1616.

[5] J.S Beck, J.C. Vartuli, W.J. Roth, M.E. Leonowicz, C.T. Kresge, K.D. Schmitt, C.T.W. Chu, D.H. Olson, E.W. Sheppard, S.B. Mccullen, J.B. Higgins and J.L. Schelnker // *J. Am. Chem. Soc.* **114** (1992) 10834.

[6] K. Moller and T. Bein // *Chem. Mater.* **10** (1998) 2950.

[7] P. Selvam, S.K. Bhatia and C. Sonwane // *Ind. Eng. Chem. Res.* **40** (2001) 3237.

[8] T. Abe, Y. Tachibana, T. Uematsu and M. Iwamoto // *J. Chem. Soc., Chem. Commun.* (1995) 1018; M. Iwamoto, T. Abe and Y. Tachibana // *J. Mol. Catal. A* **155** (2000) 143.

[9] M. Fröba, R. Kohn and G. Bouffaud // *Chem. Mater.* **11** (1999) 2858.

[10] H. Hamdan, S. Endud, H. He, M.N.N. Muhid and J. Klinowski // *J. Chem. Soc., Farad. Trans.* **92** (1996) 2311.

[11] K. Schumacher, M. Grun and K.K. Unger // *Micropor. Mesopor. Mater.* **27** (1999) 201.

[12] N.Y. He, J.M. Cao, S.L. Bao and Q.H. Xu // *Mater. Lett.* **31** (1997) 133.

[13] A. Tuel, I. Arcon and J.M.M. Millet // *J. Chem. Soc., Farad. Trans.* **94** (1998) 3501.

[14] P. Selvam, S.K. Badamali, M. Murugesan and H. Kuwano, In: *Recent Trends in Catalysis,* ed. by V. Murugesan, B. Arabindoo and M. Palanichamy (Narosa, New Delhi, 1999) p.556.

[15] S.K. Badamali and P. Selvam // *Stud. Surf. Sci. Catal.* **113** (1998) 749.

[16] S.E. Dapurkar, S.K. Badamali and P. Selvam // *Catal. Today* **68** (2001) 63.

[17] P. Selvam, S.E. Dapurkar, S.K. Badamali, M. Murugesan and H. Kuwano // *Catal. Today* **68** (2001) 69.

[18] R.D. Shannon // *Acta Crystallogr. A* **32** (1976) 751.

[19] S.K. Badamali, A. Sakhivel and P. Selvam // *Catal. Lett.* **65** (2000) 153.

[20] B. Echcahed, A. Moen, D. Nicholson and L. Bonneviot // *Chem. Mater.* **9** (1997) 1716.

[21] D. Goldfarb, M. Bernardo, K.G. Strohmaier, D.E.W. Vaughan and H.J. Thomann // *J. Am. Chem. Soc.* **116** (1994) 6344.

[22] S. Bordiga, R. Buzzoni, F. Geobalda, C. Lamberti, T.E. Giamello, A. Zecchina Leofanti, G. Petrini, G. Tozzola and G. Vlaic // *J. Catal.* **158** (1996) 486.

[23] E.G. Derouane, M. Mestdagh and L. Vielvoye // *J. Catal.* **33** (1974) 169.

[24] D.H. Lin, G. Condurier and J. C. Vedrine // *Stud. Surf. Sci. Catal.* **49** (1989) 143.